PHYSICAL REVIEW B VOLUME 60, NUMBER 11 15 SEPTEMBER 1999-I

Unusual dispersion of image potential states on the Be($\bar{1}010$) surface

V. M. Silkin
Departamento de Física de Materiales y Centro Mixto CSIC-UPV/EHU, Facultad de Química, Universidad del País Vasco, Euskal Herriko Unibertsitatea, Apartado 1072, 20018 San Sebastián/Donostia, Spain
and Institute of Strength Physics and Materials Science, Russian Academy of Sciences, pr. Academicheskii 2/1, 634021 Tomsk, Russia

E. V. Chulkov and P. M. Echenique
Departamento de Física de Materiales y Centro Mixto CSIC-UPV/EHU, Facultad de Química, Universidad del País Vasco, Euskal Herriko Unibertsitatea, Apartado 1072, 20018 San Sebastián/Donostia, Spain
(Received 12 April 1999)

We present a self-consistent pseudopotential calculation of image potential states on the Be($\bar{1}010$) surface. The one-electron potential inside the crystal and surface region is described by the local density approximation and by the image potential in the vacuum region (at $z>z_{im}$). The calculated first image state ($E_1=-1.20$ eV) lies in the symmetry gap and the second image state ($E_2=-0.31$ eV) is located inside the absolute energy gap. High anisotropy of the dispersion of both image states is found. The effective masses that reflect this anisotropy are obtained $m_1^*/m_e=1.55\pm0.1$, $m_2^*/m_e=1.30\pm0.1$ along the $\bar{\Gamma}\bar{M}$ direction and $m_1^*/m_e=0.40\pm0.05$, $m_2^*/m_e=0.55\pm0.05$ along $\bar{\Gamma}\bar{A}$. The unusual dispersion of the image states on Be(1010) is due to a large penetration value p_n of these states ($p_1=0.34$ and $p_2=0.15$), and the very anisotropic character of the symmetry energy gap edges. [S0163-1829(99)00135-6]

Anisotropic surfaces can exibit unconventional properties that can be used to study the physics of many-body interactions, including the anisotropic screening waves,[1] nontrivial dependence of dispersion and decay of surface and image states on momentum,[2,3] interactions of these states with linear and point defects.[4] Recently Ortega *et al.*[2] have observed on Cu(100) the first image state localized completely on a step with free-electronlike dispersion parallel to the step and no dispersion perpendicular to the step. Anisotropic dispersion of the first image state has also been found for indium chains on Si(111).[3] On both systems, which are drastically different from each other, the dispersion of the image state has been found to be parabolic with the free-electron mass along the dominant direction and to fall below the free-electron parabola in the perpendicular direction. Such a behavior of the electron state is directly related to artificially created anisotropy: by linear defects on Cu(100) and adsorbed indium chains on Si(111). At the same time, any influence of bulk band structure on anisotropic dispersion of the image state has not been found in Refs. 2 and 3.

In this paper, we present first-principle calculation results for image states on a naturally anisotropic surface Be(1010). We demonstrate unusual properties of these states–a very high binding energy and highly anisotropic dispersion. To our knowledge, the binding energy of the first image state on Be(1010) is significantly higher than that experimentally observed ever before on other clean metal surfaces.[5] We also show that in contrast to artificially created anisotropic surfaces[2,3] the effective mass of the $n=1$ state along the closed-packed rows exceeds significantly the free-electron mass and is considerably smaller than the free electron mass in the perpendicular direction. All these properties are directly related to the crystal anisotropy of Be(1010) and inconventional character of bulk electronic structure of Be. The key role of the anisotropy on Be(1010) has also been illustrated in Ref. 1 where highly anisotropic two-dimensional Friedel oscillations of charge density were observed.

Contrary to other simple metal surfaces, the vacuum level in Be(1010) lies inside the energy gap at the $\bar{\Gamma}$ point.[6] This can lead to existence of image potential states linked to this level.[5,7,8] According to the conventional formula[7] $E_n=-1/(n+a)^2$ the binding energy of the first image state located in such a gap falls in energy interval $0.50-0.85$ eV below the vacuum level. Experimentally the image states on various noble and transition metal surfaces have been studied by using inverse photoemission (IP),[8,9] two-photon photoemission (2PPE),[5] and time-resolved two-photon photoemission (TR2PPE).[10,11] The lowest measured energy of -0.82 eV relative to the vacuum level has been obtained for the first image state on Cu(111).[5,10] The largest effective masses m_1^*/m_e have been found to be of 1.3 ± 0.15 and 1.5 ± 0.3 for the first image state on Ag(111) (Ref. 12) and Au(100),[13] respectively. It has been also observed that m_1^* does not manifest an angle dependence.[5,12]

The (1010) surface of hcp metals can be terminated with either short or long first interlayer spacing. Clear preferance for the short first interlayer spacing termination of Be(1010) has been found both experimentally and theoretically.[14] So, this surface geometry is used in the present calculation. Figure 1 illustrates the anisotropic crystal structure of Be(1010) with closed-packed atomic rows along the x axis and the corresponding surface Brillouin zone. For the calculation of the charge density of the Be(1010) surface we use the self-consistent norm conserving pseudopotential method in a supercell geometry [the films consisting of 12 layers (6 double layers) and separated by four double layers of vacuum] within the local density approximation (LDA). We have optimized the surface geometry allowing the relaxation of the

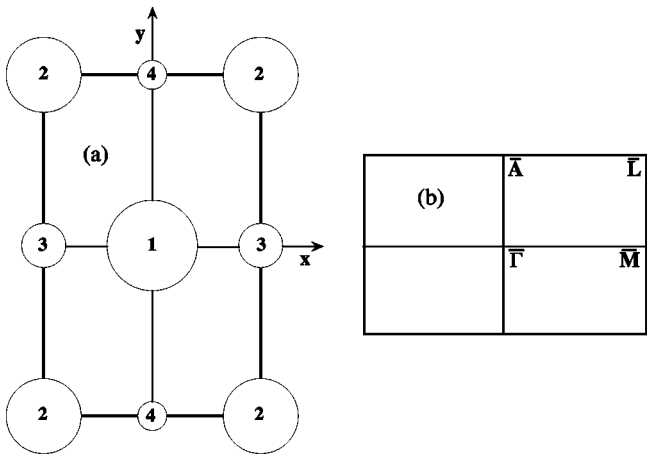

FIG. 1. (a) Unit cell of the Be($10\bar{1}0$) surface (top view). The numbers 1, 2, 3, and 4 denote the atomic positions in the first four atomic layers, respectively. (b) The surface Brillouin zone of Be($10\bar{1}0$) with the irreducible part $\bar{\Gamma}\bar{A}\bar{L}\bar{M}$.

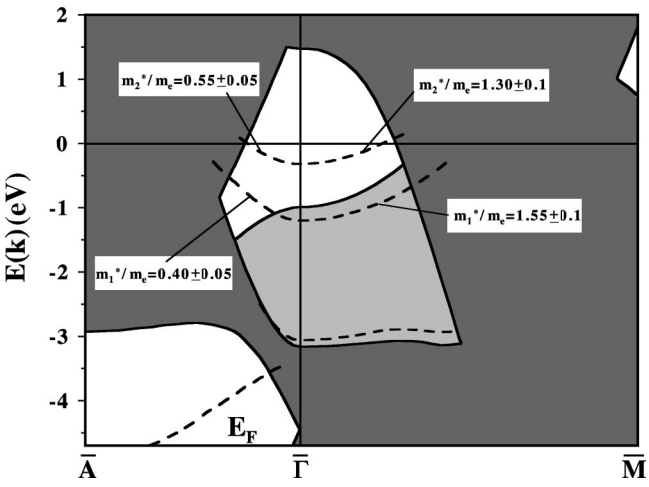

FIG. 2. Calculated surface electronic structure of Be($10\bar{1}0$) along the $\bar{\Gamma}\bar{A}$ and $\bar{\Gamma}\bar{M}$ directions: the projected band structure of bulk Be (shaded areas) and the surface and image states (dashed lines). $E_V=0$.

uppermost two atomic layers on either side of the film. The calculation gives the contraction of the first interlayer spacing by 19% and expansion of the second one by 8%. These values are in agreement with both calculated (20% and 4.4%) and experimental (25% and 5%) (Ref. 14) results for the first and second interlayer spacing, respectively.

As the LDA does not describe the correct asymptotic behavior of the potential in the vacuum region the final iteration of the self-consistent procedure is carried out by using a modified potential that for $z<z_{im}$ is the self-consistent LDA one and for $z>z_{im}$ is $V(z)=\{\exp[-\lambda(z-z_{im})]-1\}/[4(z-z_{im})]$. The damping parameter λ is a function of (x,y) and is fixed by the requirement of continuity of the potential at $z=z_{im}$ for each couple of (x,y). The image plane position z_{im} is evaluated as the center of gravity of the charge density induced by a weak static electric field. The obtained value $z_{im}=2.63$ a.u. (relative to the surface atomic layer) agrees well with pseudopotential and model potential calculations for Be(0001).[15]

With the use of the self-consistent charge density obtained for a 12-layer film we have constructed charge density for 24-layer film inserting 12 bulk layers in the center of the thin film. Vacuum space was increased from 6 double layers to 21 ones. This vacuum width is enough to describe accurately the $n=1,2$ image states. Finally, the LDA potential was generated for this new supercell with a correct imagelike behavior in the vacuum space.

The calculated unoccupied electronic structure for Be($10\bar{1}0$) along the symmetry directions $\bar{\Gamma}\bar{A}$ and $\bar{\Gamma}\bar{M}$ is shown in Fig. 2. As can be seen in the figure on Be(1010) there exists a wide energy gap at $\bar{\Gamma}$ extending from -3.15 eV up to 1.45 eV. This gap consists of two parts. The lower one (light gray color) is a symmetry gap forbidden for bulk states of s,p_z symmetry. The upper part of the gap is an absolute energy gap, which is forbidden for all bulk states. The lower edge of this part is located at -1.0 eV. Such character of the full energy gap is not the case for the most studied surfaces like low-index surfaces of noble metals[5] because it is determined by bulk states located at different points in the bulk Brillouin zone. It means that on Be(1010) the energy gap at $\bar{\Gamma}$, located at the vacuum level, is not generated by any Fourier component of the crystal potential. So, approaches that tend to describe the bulk band structure with the use of one Fourier component of the crystal potential to reproduce the energy gap are not going to be applicable to Be(1010).

As follows from Fig. 2 the surface state of the s,p_z symmetry is placed in the lower part of the symmetry gap. The charge density of this state is located mainly between the second and third atomic layers. This state appears on the relaxed surface and does not exist on the ideally terminated surface. The first image state with energy of $E_1=-1.20$ eV is located in the upper part of the symmetry gap. As this state is of s,p_z symmetry, it is not influenced by the bulk p_x,p_y states located in this part of the full gap. The second image state with energy of $E_2=-0.31$ eV is placed in the absolute energy gap. These energies are exceptionally low in comparison with corresponding values of the $n=1,2$ states on noble and transition metal surfaces.[5,7–13,16] Energies $E_1\simeq -0.9$ eV have been evaluated for close packed simple metal surfaces.[15,17,18] The electronic self-energy calculations[19] place z_{im} closer to the surface than evaluations of a linear response to external electric field do. It can influence the binding energy of image states. To estimate this influence we have calculated E_1 and E_2 with $z_{im}=2.1$ a.u. and $z_{im}=3.1$ a.u. and found that a change in z_{im} (around $z_{im}=2.63$ a.u.) of 0.5 a.u. brings a change of about 0.08 eV in E_1 and 0.02 eV in E_2. It means E_n are not very sensitive to exact position z_{im} in the 2 a.u.$<z_{im}<3$ a.u. interval. A similar slight dependence of E_1 on z_{im} was found for Be(0001), Li(100) (Refs. 15 and 17), and for Ni(100).[16]

In Fig. 3, the probability amplitudes of the first and second image states averaged in the plane parallel to the surface are shown. For comparison, we also plot the probability amplitute for an occupied surface state at $\bar{\Gamma}$.[6,14] One can see in the figure that the charge fraction of the $n=1$ state inside the crystal (the penetration) is not a small one. The total penetration value $p_1=34\%$ is significantly larger than that obtained for the first image state on noble and transition metal

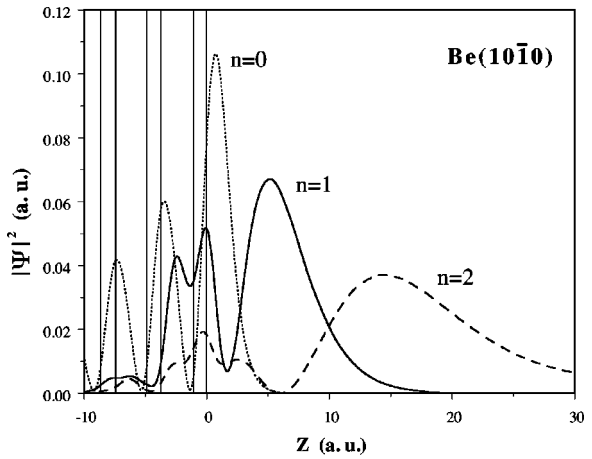

FIG. 3. The probability amplitudes averaged in the plane parallel to the surface are shown for the $n=1,2$ image states and for the occupied surface state ($n=0$). Vertical solid lines represent atomic layers positions.

surfaces. For instance, for Cu(100), Ag(100), Pd(111), Ni(100), on which image states are, like for Be(1010), in the middle of the energy gap, p_1 is about 5%.[15] At the same time the value $p_1=34\%$ is comparable with the one, $p_1=22\%$ found for the Cu(111) and Ag(111) surfaces.[15] But on these surfaces the first image state is located just below the upper edge of the energy gap. This location leads to increasing the penetration of the state compared with the state positioned in the middle of the gap.

As one can see in Fig. 3 the probability amplitude (density) of the first image state has no node in the vicinity of the geometrical edge. The node is observed for the $n=1$ state on close-packed metal and transition metal surfaces,[15,20] for which the surface corrugation effects are negligible. The Be(1010) surface has a higher corrugation than (100) and (111) surfaces of fcc metals and this corrugation determines the very anisotropic behavior of the probability amplitude of image states in the (x,y) plane. In Fig. 4, we show the probability amplitude contours for the first image state in some planes. As follows from the figure the density of the state manifests the strong dependence on x and y variables in the surface region. In this region the state forms density rows along the [0100] direction (the x axis in Fig. 1). The density shows very smooth behavior in the vacuum space beyond the geometrical edge. For each couple of (x,y) the density $|\psi(x,y,z)|^2$ has a node at different z points. A quite similar picture is observed for the second image state. The probability amplitude of this state has a node at $\simeq 6$ a.u. relative to the surface layer. At the same time there is no node in the vicinity of the geometrical edge. Again, as in the case of the $n=1$ state, this is due to the large penetration (up to 15%) and highly anisotropic character of the surface.

The large penetration of the image states on Be(10$\bar{1}$0) assumes that this surface has lower electron reflectivity than that of close-packed surfaces like Cu(100), Ag(100), Li(110), and Be(0001). The lower electron reflectivity is determined by two first surface atomic layers, because the penetration charge is mainly located between the geometrical edge and the third layer. Qualitatively this conclusion can also be made from the potential behavior in the surface region. The calculated local part of the full screened nonlocal

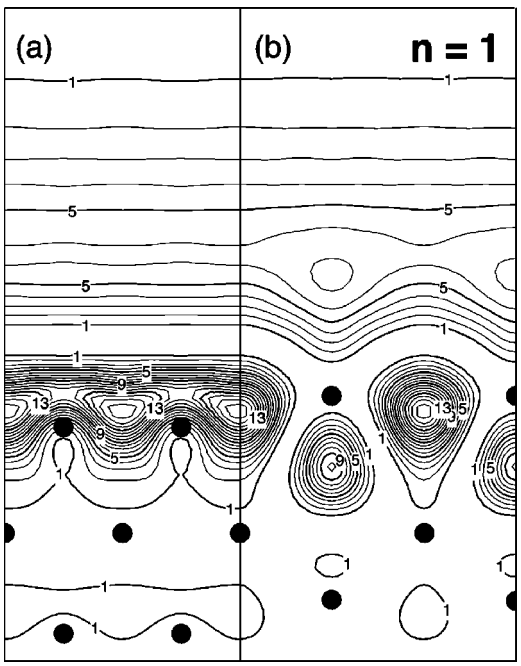

FIG. 4. Charge-density contour plots (arb. units) of the $n=1$ image state at the $\bar{\Gamma}$ points drawn in two planes, which are perpendicular to the surface and contain the atoms of (a) the second and fourth atomic layers (2-4-2), (b) the first and fourth atomic layers (4-1-4). Full circles indicate the atomic positions.

pseudopotential averaged in the plane parallel to the surface has the potential well just beyond the surface atomic layer whose depth is significantly smaller than that inside the crystal. This is in contrast with more close packed surfaces like Li(110) and Be(0001) where the potential depth beyond the surface layer is comparable with that inside the crystal.[15,17] The higher electron reflectivity of Li(110) leads to a smaller penetration value $p_1=15\%$ of the $n=1$ state.

Another unusual feature of image states on the Be(10$\bar{1}$0) surface is their highly anisotropic dispersion. This dispersion is not free-electron like and the effective mass m^* of these states changes qualitatively from one symmetry direction to another one. The first image state disperses parabolically along the $\bar{\Gamma}\bar{M}$ direction with the effective mass of $m_1^*/m_e=1.55\pm0.1$, while along $\bar{\Gamma}\bar{A}$ it is described by the effective mass of $m_1^*/m_e=0.40\pm0.05$. A similar picture is observed for the second image state. In this case the effective masses are found to be $m_2^*/m_e=1.30\pm0.1$ and $m_2^*/m_e=0.55\pm0.05$ along the $\bar{\Gamma}\bar{M}$ and $\bar{\Gamma}\bar{A}$ directions, respectively. We have not calculated the $n=3$ image state because of limitations of vacuum spacing between the films. Nevertheless, one can conclude from our results that the effective mass of, at least, the $n=3$ state should be different from the free-electron like mass, exhibiting the same anisotropic character as the $n=1,2$ states do. The very anisotropic behavior and $m_i^*\neq m_e$ for $n=1,2,3,\ldots$ have not been observed for image states on other surfaces so far studied.[5] The largest value of m_1^*/m_e has been found in 2PPE experiment for Ag(111) to be 1.3 ± 0.1 (Ref. 12) and the lowest one $m_1^*/m_e=0.9\pm0.1$ was obtained for the first image state on Cu(100).[5] Recently, Ciracci *et al.*[13] measured the dispersion of the $n=1$ image state on Au(100) with $m_1^*/m_e=1.5\pm0.3$ using IP. So, the

Be($\bar{1}\bar{0}10$) surface generates the first image state with both the largest and smallest values of effective mass simultaneously. Moreover, the $n=2$ state manifests the same character as the first image state showing large deviations from the free-electron-like behavior. This unusual dispersion may be explained using the bulk band structure arguments. It is well known that the symmetry of a state located inside an energy gap is dictated by the symmetry of the gap edges.[21] The lower and upper edges of the full energy gap on Be(1010) are of s,p_z symmetry at $\bar{\Gamma}$. The effective mass of the lower edge on going from $\bar{\Gamma}$ to $\bar{M}$ (see Fig. 2) is of the order of $10m_e$. At the same time the dispersion of the lower edge along $\bar{\Gamma}\bar{A}$ is characterized by $m_1^*/m_e \simeq 0.1$. This exceptionally anisotropic behavior of the lower edges dictates the anisotropic dispersion of the image states, which is enhanced due to the large penetration of these states into the bulk.

In conclusion, the present calculation has shown highly unusual properties of the binding energies and dispersion character of image states on Be(1010). These properties are dictated by the crystal and electronic structures of bulk Be, i.e., the image states on Be(1010) carry clear information on the bulk crystal and electronic properties of Be. The crystal structure determines the anisotropic arrangement of the Be atoms in the surface plane, which produces smaller electron reflectivity of this surface in comparison with the well studied surfaces of Cu and Ag.[5,7,8,15,17] The anisotropic behavior of the gap edges leads to the very anisotropic dispersion character of the first and second image states. To verify the obtained results it would be desirable to measure unoccupied electronic structure with the use of IP, 2PPE, or TR2PPE techniques. The discovered unusual characteristics may be of general interest for electron spectroscopies to measure unique dependence of the lifetime of the image states as a function of a momentum along different symmetry directions and to elucidate the physics of surface response and the anisotropy of this response.

We acknowledge R. Ritchie, A. Rubio, and E. Ortega for reading the manuscript and helpful discussions. This project has been supported by the Ministerio de Educación y Ciencia, Spain; the Departamento de Educación del Gobierno Vasco; and Iberdrola S.A.

[1] Ph. Hofmann *et al.*, Phys. Rev. Lett. **79**, 265 (1997).
[2] J. E. Ortega *et al.*, Phys. Rev. B **49**, 13 859 (1994).
[3] I. G. Hill and A. B. McLean, Phys. Rev. Lett. **82**, 2155 (1999).
[4] F. Theilmann *et al.*, Phys. Rev. B **56**, 3632 (1997).
[5] Th. Fauster and W. Steinmann, in *Electromagnetic Waves: Recent Development in Research*, edited by P. Halevi (Elsevier, Amsterdam, 1995), Vol. 2, p. 350.
[6] V. M. Silkin and E. V. Chulkov, Fiz. Tverd. Tela (St. Petersburg) **37**, 2795 (1995) [Phys. Solid State **37**, 1540 (1995)].
[7] P. M. Echenique and J. B. Pendry, J. Phys. C **11**, 2065 (1978); Prog. Surf. Sci. **32**, 111 (1990).
[8] F. J. Himpsel, Comments Condens. Matter Phys. **12**, 199 (1986); N. V. Smith, Rep. Prog. Phys. **51**, 1227 (1988).
[9] A. Goldmann, V. Dose, and G. Borstel, Phys. Rev. B **32**, 1971 (1985).
[10] M. Wolf, E. Knoesel, and T. Hertel, Phys. Rev. B **54**, R5295 (1996).
[11] R. L. Lingle, Jr. *et al.*, Chem. Phys. **205**, 191 (1996); I. L. Shumay *et al.*, Phys. Rev. B **58**, 13 974 (1998).
[12] K. Giesen *et al.*, Phys. Rev. B **35**, 975 (1987).
[13] F. Ciccacci *et al.*, J. Phys.: Condens. Matter **6**, 7227 (1994).
[14] Ph. Hofmann *et al.*, Surf. Sci. **355**, L278 (1996); Phys. Rev. B **53**, 13 715 (1996).
[15] E. V. Chulkov, V. M. Silkin, and P. M. Echenique, Surf. Sci. (to be published).
[16] M. Nekovee and J. E. Inglesfield, Europhys. Lett. **19**, 535 (1992).
[17] E. V. Chulkov, V. M. Silkin, and P. M. Echenique, Surf. Sci. **391**, L1217 (1997).
[18] F. Finocchi, C. M. Bertoni, and S. Ossicini, Vacuum **41**, 535 (1990); T. Fondén, S. Papadia, and M. Persson, J. Phys.: Condens. Matter **7**, 2697 (1995).
[19] I. D. White *et al.*, Phys. Rev. Lett. **80**, 4265 (1998); M. Heinrichsmeier *et al.*, Phys. Rev. B **57**, 14 974 (1998).
[20] S. L. Hulbert *et al.*, Phys. Rev. B **33**, 760 (1986).
[21] E. W. Plummer and W. Eberhardt, Adv. Chem. Phys. **49**, 533 (1982); F. J. Himpsel, Adv. Phys. **39**, 1 (1983).